ORIGINAL ARTICLE

Software News and Updates

# TS-tools: Rapid and Automated Localization of Transition States based on a Textual Reaction SMILES Input

**Thijs Stuyver PhD**[1*]

[1]Ecole Nationale Supérieure de Chimie de Paris, Université PSL, CNRS, Institute of Chemistry for Life and Health Sciences, 75 005 Paris, France

**Correspondence**
Thijs Stuyver PhD, Ecole Nationale Supérieure de Chimie de Paris, Université PSL, CNRS, Institute of Chemistry for Life and Health Sciences, 75 005 Paris, France
Email: thijs.stuyver@chimieparistech.psl.eu

**Funding information**
French National Agency for Research (ANR), ANR-22-CPJ1-0093-01

Here, TS-tools is presented, a Python package facilitating the automated localization of transition states (TS) based on a textual reaction SMILES input. TS searches can either be performed at xTB or DFT level of theory, with the former yielding guesses at marginal computational cost, and the latter directly yielding accurate structures at greater expense. On a benchmarking dataset of mono- and bimolecular reactions, TS-tools reaches an excellent success rate of 95% already at xTB level of theory. For tri- and multimolecular reaction pathways – which are typically not benchmarked when developing new automated TS search approaches, yet are relevant for various types of reactivity, cf. solvent- and autocatalysis and enzymatic reactivity – TS-tools retains its ability to identify TS geometries, though a DFT treatment becomes essential in many cases. Throughout the presented applications, a particular emphasis is placed on solvation-induced mechanistic changes, another issue that received limited attention in the automated TS search literature so far.

KEYWORDS
*transition states*, *automation*, DFT, SMILES, xTB

## 1 | INTRODUCTION

Automating and accelerating reaction pathway exploration and transition state (TS) localization remains an outstanding challenge in computational chemistry. Various approaches have been proposed and developed to this end in recent years, each with their specific advantages and limitations. Providing a full overview of all the developed methods and codes is beyond the scope of this work; we refer to some excellent reviews on this topic for further reading. [1, 2, 3, 4] *Grosso modo*, one can distinguish single-/open- and double-ended approaches. The former, e.g., the artificial force-induced reaction (AFIR) method, [5, 6, 7] the imposed activation method, [8] Chemoton [9, 10], the reaction mechanism generator (RMG), [11] the chemical discovery engine (CDE), [12] and the nanoreactor, [13, 14] are typically designed for exhaustive reaction mechanism exploration efforts, i.e., they compute multiple reaction pathways simultaneously, and consequently, they tend to require extensive computational resources to treat even a single combination of reactants. Strategies have been explored to speed up such open-ended exploration efforts with remarkable success, cf. the YARP method – which in its turn is based on an exhaustive molecular graph editing approach in combination with the double-ended growing string method (GSM) algorithm [15, 16] – developed by Savoie and co-workers among others, [17, 18] but this usually requires the adoption of stringent limitations to the type of reactions that can be considered, to reign in the combinatorial explosion of reaction possibilities as reactants grow bigger. [19] Double-ended approaches only consider a single reaction pathway at a time, and hence they enable in principle more rapid mechanistic investigations – under the condition that the reaction pathways of interest can straightforwardly be identified *a priori* – and/or they facilitate the generation of more refined, i.e., more accurate, reaction profiles on a limited computational budget (for example by performing more exhaustive conformational searches), e.g., autodE [20] and the RMSD-PP method. [21, 22]

A notable limitation of most TS search methods developed up to this point – with a few exceptions, cf. AFIR [5, 6, 7] – however is that they have been primarily designed for – and validated on – mono- and bimolecular reactions. This despite the unequivocal demonstration that reaction pathways involving more than two reaction partners are ubiquitous and relevant in many important chemical processes as well, cf. autocatalysis, [23, 24] solvent-catalyzed reactions, e.g., tautomerization, [25, 26, 27, 28] and enzymatic reactivity (Fig. 1). [29] The difficulty in straightforwardly adapting most TS search algorithms to locate such multi-species mechanisms limits their practical usefulness in reaction mechanism explorations for many reaction types. Another issue that has received limited attention so far in the literature related to automated TS search algorithms is the impact of reaction conditions on mechanistic landscapes. Indeed, benchmarkings and simulations across the research field are typically exclusively performed in gasphase, even though it has been well documented that taking solvent environments into account not only affects the relative energetics of reaction paths, but can also result in the emergence of new – as well as the disappearance of old – pathways. [30, 24, 31]

It should also be noted that recently, algorithms for automated TS localization have emerged as generators of training data for machine learning (ML) based reactivity models. [33, 34, 35, 36, 37, 38, 39, 40, 41] As such, these algorithms are rapidly becoming an indispensable tool for setting up ML accelerated workflows for reaction discovery and development. Consequently, one can expect a bias in the types of reactivity that can be treated accurately by these TS search methods to also seep into downstream ML models. This underscores the continued need to explore new algorithms and approaches to identify truly diverse reaction pathways under diverse conditions.

In this manuscript, a compact and user-friendly Python module, enabling rapid localization of TS (guesses), resulting from the rapprochement of one or more reactants based on textual (atom-mapped) reaction SMILES [42] input is presented. Basing our approach on a reaction SMILES input makes it inherently compatible with graph-based reaction generation algorithms, which are commonly used in ML-based predictive reactivity models, [43] and could thus be en-

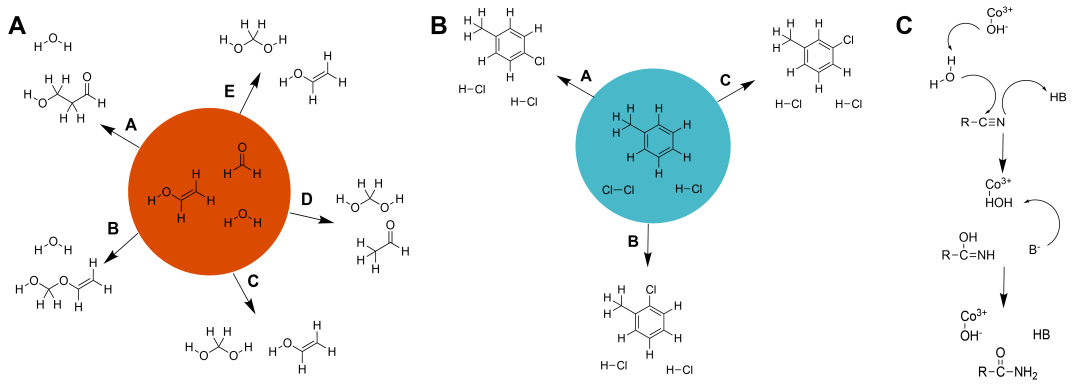


**FIGURE 1** (A) An example of a solvent-catalysis: the reaction network associated with the aldol reaction between vinyl alcohol, formaldehyde and water; (B) an example of an autocatalysis: the electrophilic aromatic substitution reaction between toluene and $Cl_2$, where the product molecule HCl participates in the formation of more energetically favorable TS structures; (C) an example of a (proposed) multi-molecular mechanism for a prototypical enzymatic reaction: nitrile hydrolysis at the $Co^{3+}$ site of Co-NHase. [32]

visioned to become an integral part of a future exhaustive reaction mechanism enumeration software package. At its core, our approach is inspired by the AFIR method, but instead of a single-/open-ended search based on randomly generated initial complex geometries, we generate reactive complexes by aligning reactant and product structures, in a similar manner as in the YARP and Chemoton codes, [17, 10] before applying the artificial force along the bonds being formed throughout the reaction – as determined from the reaction SMILES. A final element of our approach is the use of semi-empirical electronic structure methods, more specifically Grimme's extended tight-binding (xTB) method, [44] to generate reaction paths, and optionally full-fledged TS guesses, which speeds up the algorithm significantly compared to a full DFT treatment. As demonstrated below, the latter does not compromise significantly the success rate for many common reaction types.

The outline of the remainder of this paper is as follows. First, a more in-depth outline of the implemented code will be provided, and its ability to recover elementary (mono- and bimolecular) reactions in an established benchmarking dataset will be demonstrated. Subsequently, the usefulness of the algorithm in the exploration of trimolecular reactions will be illustrated by considering a small representative set of relevant applications. In these applications, we focus particularly on the effect of taking correct solvation conditions into account. Finally, some limitations and an outlook on future improvements/envisioned expansions will be critically discussed.

## 2 | DESCRIPTION OF THE TS-TOOLS CODE

At its core, the TS-tools code is built around two Python classes: PathGenerator and TSOptimizer. Below, the methodology of both objects will be discussed, after which an overview of the custom run-scripts included in the TS-tools code will also be provided. In Fig. 2, a schematic overview of the full TS search strategy is provided.

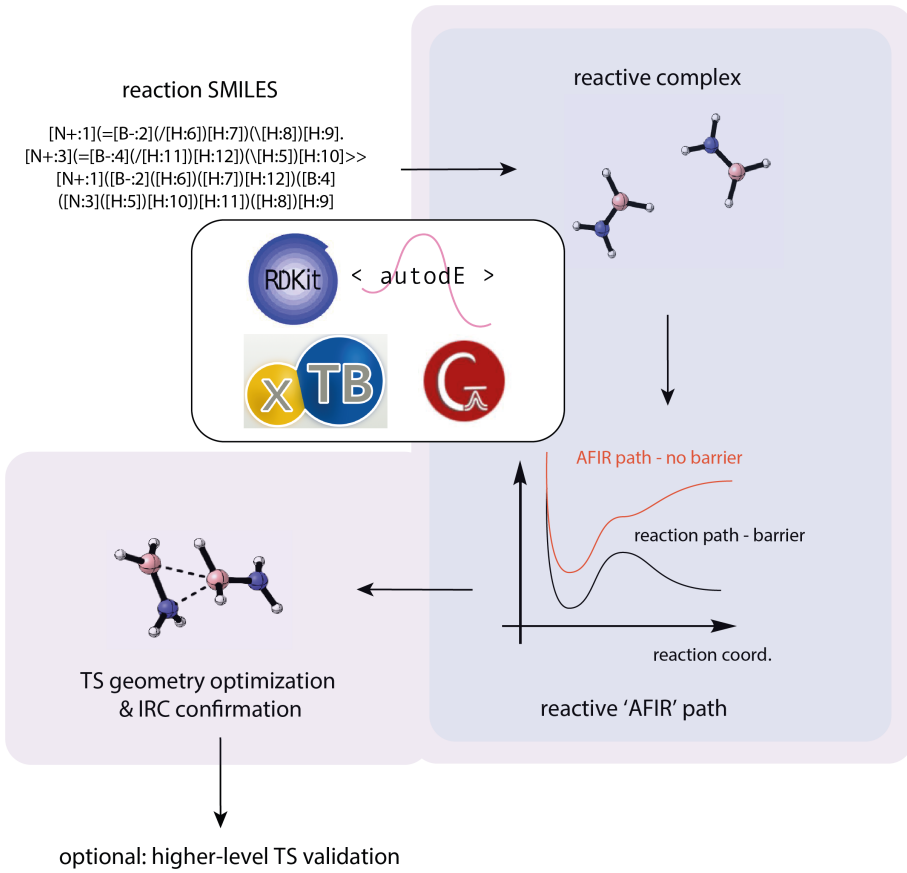


**FIGURE 2** A schematic overview of a TS-tools-based TS search. The part of the workflow covered by the PathGenerator is shaded in purple; the part covered by the TSOptimizer is shaded in pink. The code makes use of RDKit, [45] autodE, [20] xTB [21] and Gaussian16.[46]

## 2.1 | PathGenerator

The workflow associated with the PathGenerator object starts by generating an initial reactive complex. To this end, reactant and product SMILES are compared, and 'active bonds' that change throughout the reaction are identified with the help of RDKit. [45] Subsequently, optimal bond lengths are determined for every active bond defined in the SMILES for individual reactant and product molecules. Next, an initial conformer is generated with the help of autodE's *randomize-and-relax* algorithm, [20] in which the bond ideal lengths on the reactant-side are enforced, and additional constraints are set to the bonds being formed throughout the reaction: they get assigned the ideal bond length on the product side, multiplied by a (parameterized) stretch factor, to which a random modulating factor is added to induce some variability in the geometries of the generated complexes. Taking this approach, the reactants are pre-organized to facilitate the smooth transition from reactant to product geometry. If the stereochemistry of the generated conformer is not compatible with the stereochemistry in the reactant SMILES, then the *randomize-and-relax* procedure is repeated until the latter condition is fulfilled (or until 100 conformers with an incorrect stereochemistry have been generated). The resulting stereocompatible conformer is subsequently optimized at xTB level of theory,

[44] where the constraints on the forming bonds are set with small force constants.

In the next step, reactive (AFIR) paths [5] are generated for the (relaxed) reactive complexes. To this end, a biased optimization is run on the reactant complex geometry, where constraining (harmonic) potentials are applied to the forming bonds, with an optimal distance corresponding to the respective ideal product bond lengths. The PathGenerator aims to find the lowest force constant required for the external potentials to facilitate access to the product region of the potential energy surface (PES), as small force constants reduce the odds of visiting regions of the unbiased PES that are unrealistically high in energy. In other words, they reduce the risk of drifting far away from the saddle point connecting the reactant and product valleys, i.e., they improve the chance of sampling the actual transition state region. [5]

To determine the minimal value needed to push the molecular system from the reactant to the product valley in the PES, the force constant is increased by stepsize 0.1 au (Hartree/Bohr$^2$) in first instance. At every step, the value of the total external potential at the end of the biased optimization is compared to a small threshold value. As soon as the threshold is reached, indicating that the product geometry is obtained for the considered force constant, a more refined search is performed within the window of the last force constant step. More specifically, force constant values are now gradually increased by 0.01 au increments, starting from the second to last value tried during the first phase of the search. Once the external potential reaches the threshold value anew, a final refinement of the force constants is performed with a stepsize of only 0.001 au. Since the external potential values can become extremely low in this final refinement phase, the external potential threshold is complemented with a comparison between the product connectivity (as defined in the SMILES string) and the connectivity of the optimized structure, to gauge the success of the reactive path search at this stage. Up to five paths, each starting from a (re-)initialized reactive complex, are generated in this final refinement. As soon as a successful path is detected, the intermediate geometries and associated energies visited throughout the optimization are extracted and saved as the reactive path retained for further examination.

## 2.2 | TSOptimizer

The workflow associated with the TSOptimizer object starts by determining a reactive path for a defined stretching factor, i.e., it involves the generation of a PathGenerator object (*vide supra*). If during the initialization of the latter object, the number of bonds being formed is detected to be smaller than the number of bonds being broken, then the direction of the reaction is reversed by default for intramolecular reactions, to facilitate the generation of correct reactive paths.

Subsequently, unbiased energy values are determined for every frame along the reaction path by subtracting the external potentials from the energies outputted during the biased optimization. Local maxima in terms of unbiased energy along the generated path are then selected as candidate TS guesses. A crude filtering is applied in this step to remove local minima that stand no chance of resembling the actual transition state. More specifically, local maxima for which the corresponding geometry yields an imaginary frequency below 150 cm$^{-1}$ and/or an imaginary mode for which the main displacement does not correspond to an active bond – as computed with xTB – are rejected. The local maxima are subsequently ranked according to their energies, and the 5 highest-energy ones are then successively used as input for a Gaussian16 [46] transition state optimization.

With the help of TS-tools, Gaussian16 TS optimization can be performed either at xTB or DFT level of theory (the former is made possible through the *xtb_guassian*-script from the Jensen lab). [47] By default, a TS optimization is always followed by an IRC confirmation at the same level of theory, since this constitutes the most reliable tool to validate that the correct TS has been found. [22] If the (re-optimized) end-points of the TS search yield the same

connectivity, as gauged with the help of *autodE*, [20] as the begin- and end-point of the retained reactive path, then the TS is assumed to be correct. As soon as a correct TS is encountered, iteration through the local maxima is halted, and the final geometry is returned.

### 2.3 | Run scripts

Three generic run scripts, which build on the PathGenerator and TSOptimizer objects, have been included in the current version of the TS-tools package. The *run_ts_searcher.py* script takes as input a *.txt* file and generates (validated) TS geometries at xTB level-of-theory. To this end, it iterates through a set of stretching factors to generate reactive complexes, and runs the TSOptimizer workflow. As soon as a validated transition state is obtained, the final geometry, as well as the geometries of the begin- and end-points of the reactive path that resulted in this TS are saved. The *run_dft_validation.py* script refines the TS geometries from xTB to DFT level of theory. Since xTB TS geometries are typically good estimates for the DFT TS geometries, Gaussian16 [46] usually reaches convergence in just a handful of iterations in this manner. As such, successively applying both scripts described so far is the fastest way to obtain DFT quality transition states in TS-tools.

Alternatively, the *run_ts_searcher_dft.py* script can be used to generate TS geometries at DFT level of theory directly from reactive paths generated with xTB. While the latter approach is significantly slower, it often times leads to the successful location of the TS when the xTB to DFT refinement approach fails (*vide infra*).

## 3 | BENCHMARKING THE PERFORMANCE OF TS-TOOLS

As a first test to probe the performance of TS-tools, we turned to the benchmarking reaction dataset proposed by Zimmerman et al. [48, 49] As demonstrated by Jensen and co-workers, this dataset of 100 mono- and bi-molecular reactions contains some errors, i.e., reactions that are not elementary. [22] Additionally, some reactions involve SMILES that RDKit cannot parse straightforwardly. As such, a cleaned-up version of this dataset has been curated as part of this study (cf. Section S1 in the Supporting Information). Passing the resulting 86 curated reactions through our workflow (and using the settings described in Section S2), correct guesses are obtained for 82 of them at xTB level of theory, corresponding to a success rate of over 95%. Visual inspection of the 4 failures indicates that the employed AFIR path approach sometimes struggles to identify the correct saddle point/imaginary mode when complex rearrangements of the atoms are needed to transform reactant into product geometries (cf. Fig. 3). The full xTB level workflow is extremely fast: over 80% of the TS geometries are found and validated within 5-10 minutes on 2 CPU cores; the longest (failed) TS search lasted for 1.5 hours (cf. Section S3 for the specifications of the computing infrastructure used).

Of the 82 xTB level TSs obtained, 75 passed DFT level validation (following previous work on this dataset, UB3LYP/6-311G** was selected as the functional/basis set combination). [48, 49] Because of the quality of the xTB TS guesses, the DFT level TS searches typically converge in a couple of iterations, [17] so that all calculations finished in less than 6 hours (with an allocation of 8 CPUs each). The 7 failures are readily recovered when the TS search is retried from scratch at DFT level of theory, albeit at a much higher computational cost (the longest TS search now lasted for almost 12 hours on 8 CPUs; cf. Section S4).

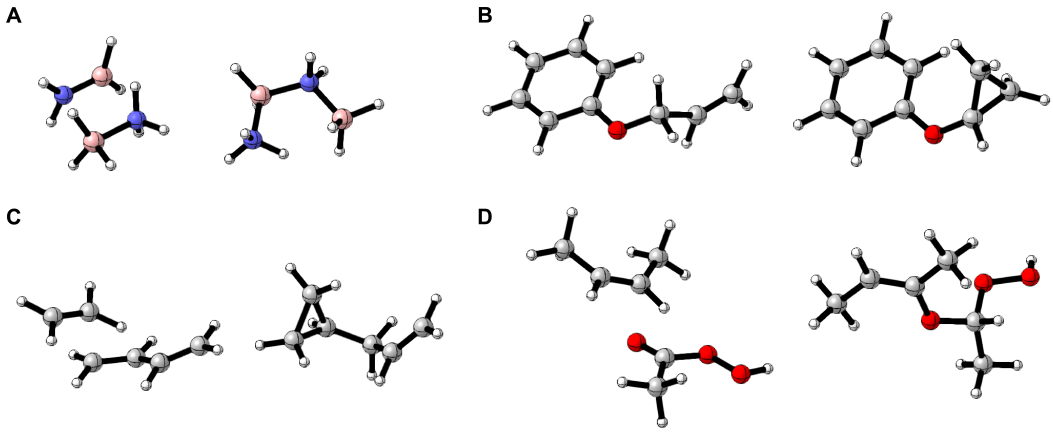


**FIGURE 3** Reactive reactant (left) and product (right) complexes for the failed reactions from the benchmarking dataset: (A) R8, (B) R98, (C) R82 and (D) R101. [50]

## 4 | APPLICATIONS

### 4.1 | Aldol Reaction

As a first test of the ability of the TS-tools approach to treating three- (and multi-)component reactions, we aimed to locate TS geometries for 5 reaction pathways associated with the aldol reaction, which constitutes a popular carbon–carbon bond formation strategy in organic chemistry. Reaction SMILES were constructed for all pathways involving vinyl alcohol, formaldehyde and water, as previously characterized by Maeda and co-workers. [51]

It should be noted that in their original work, Maeda an co-workers did not take solvent effects into account; effectively modeling the reactions in the gasphase. Adopting the same solvent-free conditions, all 5 (previously reported) TSs are readily recovered at xTB – and successfully validated at DFT – level of theory by TS-tools (cf. Fig. 4). The xTB TS searches were completed in approximately 15 min (2 CPUs were used per calculation). DFT validation finished in approximately half an hour (8 CPUs per calculation).

When a more realistic water environment is (implicitly) taken into account through the SMD polarizable continuum solvent model, [52, 53] 4 out of 5 TSs, corresponding to pathways A-D, are recovered at xTB level of theory. Unfortunately, 2 out of the 4 xTB level guesses, i.e., those associated to pathways C and D, do not survive DFT validation any longer. Performing the TS search entirely at DFT level readily recovers all guesses (cf. Fig. 5), albeit at a significant computational cost (up to 14 hours on 8 CPUs each).

Analysis of the TS associated with pathway E reveals the likely cause for its more difficult localization in an aqueous environment. Visually, one can straightforwardly observe a much higher degree of asynchronicity in the bond formation/breaking events. Additionally, the magnitude of the imaginary frequency – calculated at DFT level of theory – has been reduced dramatically compared to the gasphase TS, from 1098 $cm^{-1}$ to 571 $cm^{-1}$, indicating a much wider reaction barrier. [54] Both of these observations can be connected to the growing inter-mixing of charge transfer states along concerted reaction pathways in increasingly polar environments, as discussed at length in previous conceptual work. [55, 56] In extreme cases, such intermixing can result in mechanistic cross-over, whereby a single, concerted TS breaks down into multiple TSs separated by stable – ionic – intermediates (see for example the example in the subsection below). [24, 57, 31] It appears that for the considered transition states in this subsection, this tipping

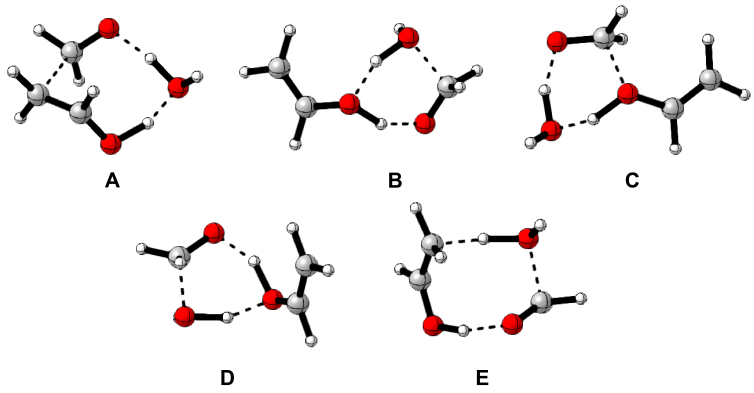


**FIGURE 4** Transition states found for the aldol reaction between vinyl alcohol, formaldehyde and water in the gasphase. The indices correspond to the respective pathways in Fig. 1a with which the TS are respectively associated. [50]

point is approached, but has not yet been crossed.

## 4.2 | Electrophilic aromatic substitution reactions in apolar and polar environments

Next, we considered the ability of TS-tools to rapidly recover the TSs for 5 pathways associated with the electrophilic aromatic substitution reaction between toluene and $Cl_2$. As repeatedly demonstrated in the literature through computational means, in apolar environments, this reaction adheres to a surprisingly complex, autocatalyzed mechanism. More specifically, we selected the pathways identified in reference [23] (cf. Fig S1 in the Supporting Information). 3 of these pathways are fully concerted (so one TS is associated with each); the final two are stepwise and involve two TSs each.

A full xTB search yields only 3 out of the 7 attempted TSs. Direct DFT optimization of the preliminary guesses from the reactive paths, however, results in the recovery of 5 out of 7 TSs (cf. Fig. 6; all successful TSs were located within 12h). Failure for the final two reactions is not surprising, since their expected structures are not so different from the geometries for some of the successfully located TSs. Consequently, even slight inaccuracies in the (preliminary) TS guesses derived from the reactive path will result in the optimization procedure leading toward an incorrect TS. Remedying these errors would likely require a more accurate topology of the reactive path than what can be achieved here with xTB.

In polar environments, the mechanism of electrophilic aromatic substitution reactions is of course very different; under these reaction conditions, an ionic Wheland intermediate is typically formed (cf. Fig. 7A). [23, 24] TS-tools readily yields the transition state leading from the reactants to this intermediate at xTB level of theory, but DFT validation fails (and so does a full DFT search). This failure can be attributed to an interfering normal mode corresponding to the rotation of the methyl group of toluene: for the simplified benzene + $Cl_2$ reacting system, the TS is found at both xTB and DFT level of theory without any problem (Fig. 7B).

Note that, by definition, a second TS is associated with the Wheland intermediate as well. It is however known from the literature that the latter TS involves the migration of the $Cl^-$ species from one side of the plane, formed by the aromatic ring, to the other. [23, 24] Since the latter cannot be described as a regular bond formation/breaking event in our SMILES-based approach, we did not try to model this here.

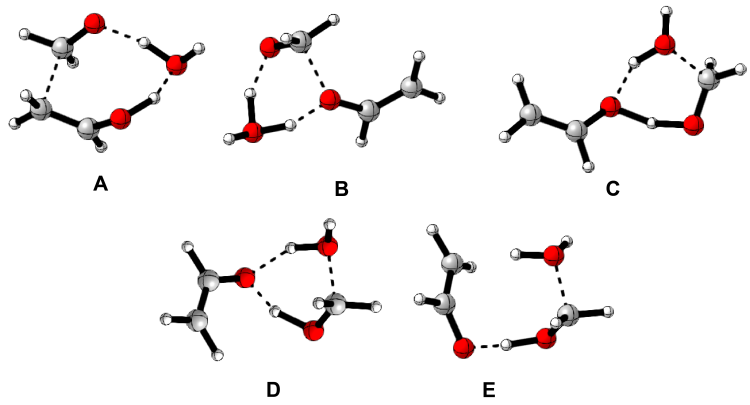


**FIGURE 5** Transition states found for the aldol reaction between vinyl alcohol, formaldehyde and water in aqueous solution. The indices correspond to the respective pathways in Fig. 1a with which the TS are respectively associated. [50]

### 4.3 | Passerini reaction

Finally, we applied TS-tools to the Passerini reaction, another iconic example of a solvent-catalyzed reaction. Three elementary reaction steps, determined in the absence of solvent effects, were once more selected from previous work by Maeda and co-workers. [51] With default settings of TS-tools, only a single TS is recovered at xTB level of theory (R2 in Fig. 8A). Lowering the increments of the final force constant refinements from 0.001 to 0.0002 au however, yields a second TS guess (R1 in Fig. 8A), though the latter does not survive subsequent DFT validation. All calculations were finished within 3.5 hours (on 2 CPUs). A full DFT search yields 2 TSs (R2 and R3); their geometries are shown in Fig. 8B. At this level of theory, the successful TS searches lasted for 12 and 14 hours respectively (the failed TS ran for 2.5 days). Once more, solvent effects affect the mechanistic landscape; only the most robust TS, i.e., R2 in Fig. 8A, is recovered when implicit solvation is taken into account (cf. Section S6).

## 5 | CONCLUSIONS & OUTLOOK

Here, we have presented a new code for automated transition state localization, TS-tools. TS-tools takes as input a simple textual reaction SMILES input and can generate the corresponding transition state structure guesses at either xTB or DFT level of theory. The presented approach exhibits excellent performance already at xTB level of theory on a common benchmarking dataset of mono- and bimolecular reaction pathways, locating good guesses for 95% of TSs in a matter of CPU minutes, 90% of which survive DFT validation and are thus of excellent quality. This superb performance suggests that TS-tools could be used for high-throughput mechanism evaluation and ML training data generation for these reaction types.

For more challenging trimolecular reaction pathways, TS-tools unequivocally retains its usefulness as an aid to rapidly and automatically identify TS guesses, but optimized xTB guesses are now significantly less accurate approximations of the actual TSs, particularly when solvent environments are taken into account. In most of the advanced applications considered, expensive DFT optimization of the preliminary guesses from the xTB reactive path was necessary to obtain validated TSs. The observation that the accuracy of semi-empirical methods such as xTB is reduced

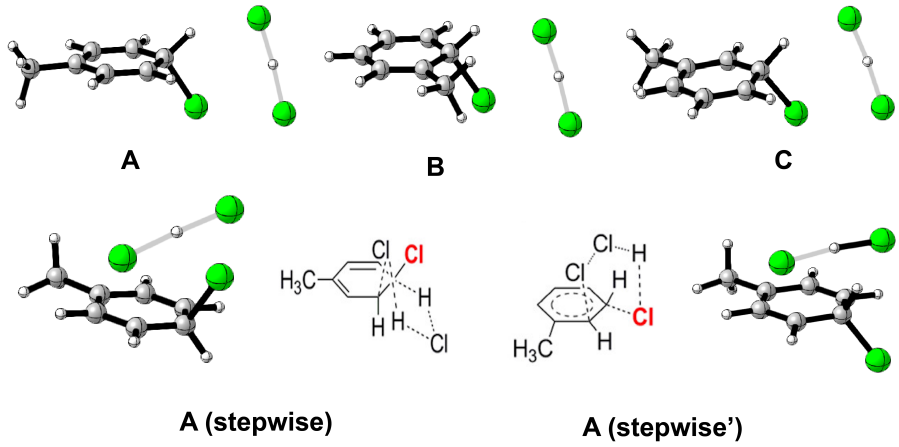


**FIGURE 6** Transition states found for the electrophilic aromatic substitution reaction between toluene and $Cl_2$, catalyzed by a single HCl molecule. The indices correspond to the respective pathways in Fig. 1a with which the TS are respectively associated. At the bottom, two alternative stepwise realizations of pathway A presented. As discussed above, for both pathways, only a single TS was found, since the other optimized towards previously found TSs (the approximate structures of those TSs are drawn here for clarity). [50]

considerably in these situations is relevant not only for the presented work, but also for other TS search algorithms making use of xTB. [17, 20, 58]

Based on the description above, it should be clear that TS-tools would first and foremost benefit from further improvements in semi-empirical electronic structure methods (and their associated implicit solvation models). New generations of these methods will hopefully result in an improved description of the PES associated with the considered reaction systems, resulting in the generation of more realistic reactive paths, and consequently a faster convergence of subsequent DFT-level TS validations. Machine learning may lead to significant advancements in this aspect in the long run, through the development of accurate neural network potentials (NNP), [59] which could potentially replace more traditional – and, as it stands, more robust – methods such as xTB. [60] In this regard, it is important to note once again that reaction mechanisms are strongly affected by their respective solvent environments – as demonstrated on several occasions throughout this manuscript – and consequently, a truly universal NNP should have the capacity to

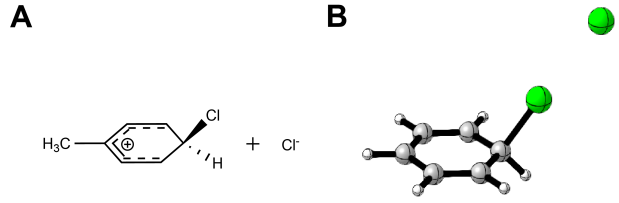


**FIGURE 7** (A) The (charge-transfer) Wheland intermediate for toluene and $Cl_2$ emerging in polar environments; (B) the TS leading the Wheland intermediate for benzene and $Cl_2$ (in this search, the intermolecular distance constraint was adjusted to 4Å, the basis set was increased to 6-31++G**, and the frequency cut-off during preliminary guess filtering was reduced to 30 $cm^{-1}$, to take the extreme width of this charge-transfer induced TS into account; water was chosen as the prototypical polar SMD solvent). [50]

https://doi.org/10.26434/chemrxiv-2024-st2tr **ORCID:** https://orcid.org/0000-0002-8322-0572 

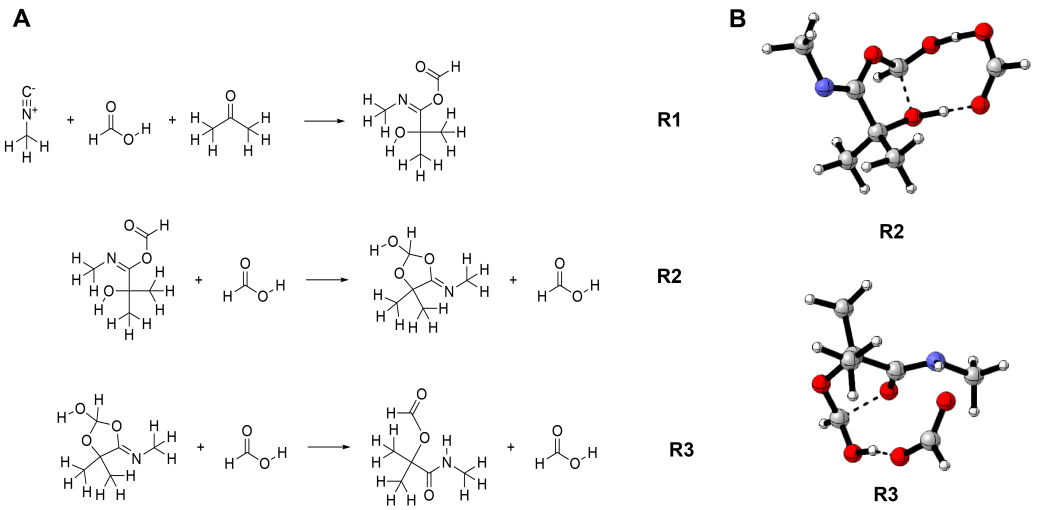


**FIGURE 8** (A) The elementary reaction steps associated with the Passerini reaction, as determined by Maeda and co-workers. [51] (B) The corresponding transition states found with TS-tools. [50]

account for this.

Next to new methods to generate reactive paths, several other opportunities to speed up and improve the algorithm can be foreseen, particularly by finetuning the selection procedure of preliminary TS guesses. Dramatic speed-ups could be achieved in this manner since most CPU time is currently spent on unsuccessful saddle-point optimizations. Selection could for example be performed by an ML agent that judges the chance of success of the downstream DFT calculations based on geometric features of the individual reactive path frames; related ideas to employ ML models to preempt unproductive calculations have recently been explored by other research groups. [61]

A similar ML-based strategy could be taken during the generation of initial reactive complex poses. Currently, a random modulating factor is included when setting non-bonded optimal distances in these complexes, and a couple of attempts are usually needed to facilitate the construction of a successful path connecting reactants and products. One can envision that an ML model trained on previous data may speed up this process by predicting distance constraints that maximize the odds of successful reactive path generation. [62]

Additions and improvements to the code that will be considered in the short to medium run are for example the introduction of a feature to construct reactive complexes through the combination of .xyz-files for individual reactant and product molecules. By enabling alternatives to the current SMILES input, TS-tools would become applicable to a much more diverse range of chemistries, e.g., transition metal chemistry – which is crucial to describe mechanistic pathways in most enzymes – as well as exotic boding situations such as compounds containing 3-center-2-electron bonds. Additionally, we will aim to explore more refined schemes to assign the external potentials, with the hope of being able to capture the handful of failed TSs in the benchmarking dataset as well (cf. Fig. 3). Finally, we also intend to introduce a feature to detect the emergence of ionic intermediates: if a reactive path yields other minima than the pre-defined product, that oftentimes means that a stable species is formed along the concerted reaction pathway due to the emergence of a charge-transfer state. Automatic detection of such intermediates could accelerate the identification of entire elementary reaction sequences, similar to those presented in the work by Maeda et al. for the original AFIR method. [5]

## acknowledgements

TS acknowledges the French National Agency for Research (ANR) for a CPJ grant (ANR-22-CPJ1-0093-01).

## Conflicts of interest

There are no conflicts to declare.

## Supporting Information

Cleaned up version of the mono-/bimolecular reaction benchmarking dataset, settings of the TS searches performed, transition state searches with failed validation, reaction profiles for the reaction between toluene and $Cl_2$ in apolar environments, note about the modeling of the solvated Passerini reaction. The main code used to generate the presented results can be found at `https://github.com/chimie-paristech-CTM/TS-tools`. The final gaussian16 outputs of all electronic structure calculations, as well as .xyz files for reactive complexes and optimized TSs, can be downloaded from `https://doi.org/10.6084/m9.figshare.25043918`.

## references

[1] Unsleber JP, Reiher M. The exploration of chemical reaction networks. Annu Rev Phys Chem 2020;71:121–142.

[2] Habershon S. Automated prediction of catalytic mechanism and rate law using graph-based reaction path sampling. J Chem Theor Comput 2016;12(4):1786–1798.

[3] Dewyer AL, Argüelles AJ, Zimmerman PM. Methods for exploring reaction space in molecular systems. Wiley Interdiscip Rev Comput Mol Sci 2018;8(2):e1354.

[4] Simm GN, Vaucher AC, Reiher M. Exploration of reaction pathways and chemical transformation networks. J Phys Chem A 2018;123(2):385–399.

[5] Maeda S, Harabuchi Y, Takagi M, Taketsugu T, Morokuma K. Artificial force induced reaction (AFIR) method for exploring quantum chemical potential energy surfaces. Chem Rec 2016;16(5):2232–2248.

[6] Sameera W, Maeda S, Morokuma K. Computational catalysis using the artificial force induced reaction method. Acc Chem Res 2016;49(4):763–773.

[7] Maeda S, Harabuchi Y. Exploring paths of chemical transformations in molecular and periodic systems: An approach utilizing force. Wiley Interdiscip Rev Comput Mol Sci 2021;11(6):e1538.

[8] Lavigne C, Gomes G, Pollice R, Aspuru-Guzik A. Guided discovery of chemical reaction pathways with imposed activation. Chem Sci 2022;13(46):13857–13871.

[9] Simm GN, Reiher M. Context-driven exploration of complex chemical reaction networks. J Chem Theor Comput 2017;13(12):6108–6119.

[10] Unsleber JP, Grimmel SA, Reiher M. Chemoton 2.0: Autonomous exploration of chemical reaction networks. J Chem Theor Comput 2022;18(9):5393–5409.

[11] Gao CW, Allen JW, Green WH, West RH. Reaction Mechanism Generator: Automatic construction of chemical kinetic mechanisms. Comput Phys Commun 2016;203:212–225.

[12] Habershon S. Sampling reactive pathways with random walks in chemical space: Applications to molecular dissociation and catalysis. J Chem Phys 2015;143(9).

[13] Wang LP, Titov A, McGibbon R, Liu F, Pande VS, Martínez TJ. Discovering chemistry with an ab initio nanoreactor. Nat Chem 2014;6(12):1044–1048.

[14] Martínez TJ. Ab initio reactive computer aided molecular design. Acc Chem Res 2017;50(3):652–656.

[15] Zimmerman PM. Growing string method with interpolation and optimization in internal coordinates: Method and examples. J Chem Phys 2013;138(18).

[16] Zimmerman PM. Single-ended transition state finding with the growing string method. J Comput Chem 2015;36(9):601–611.

[17] Zhao Q, Savoie BM. Simultaneously improving reaction coverage and computational cost in automated reaction prediction tasks. Nat Comput Sci 2021;1(7):479–490.

[18] Zhao Q, Savoie BM. Algorithmic explorations of unimolecular and bimolecular reaction spaces. Angew Chem, Int Ed 2022;134(46):e202210693.

[19] Unsleber JP. Accelerating Reaction Network Explorations with Automated Reaction Template Extraction and Application. J Chem Inf Model 2023;.

[20] Young TA, Silcock JJ, Sterling AJ, Duarte F. autodE: automated calculation of reaction energy profiles—application to organic and organometallic reactions. Angew Chem, Int Ed 2021;133(8):4312–4320.

[21] Grimme S. Exploration of chemical compound, conformer, and reaction space with meta-dynamics simulations based on tight-binding quantum chemical calculations. J Chem Theor Comput 2019;15(5):2847–2862.

[22] Rasmussen MH, Jensen JH. Fast and automatic estimation of transition state structures using tight binding quantum chemical calculations. PeerJ Phys Chem 2020;2:e15.

[23] Galabov B, Nalbantova D, Schleyer PvR, Schaefer III HF. Electrophilic aromatic substitution: new insights into an old class of reactions. Acc Chem Res 2016;49(6):1191–1199.

[24] Stuyver T, Danovich D, De Proft F, Shaik S. Electrophilic aromatic substitution reactions: Mechanistic landscape, electrostatic and electric-field control of reaction rates, and mechanistic crossovers. J Am Chem Soc 2019;141(24):9719–9730.

[25] Gu J, Leszczynski J. A DFT study of the water-assisted intramolecular proton transfer in the tautomers of adenine. J Phys Chem A 1999;103(15):2744–2750.

[26] Markova N, Enchev V, Timtcheva I. Oxo- hydroxy tautomerism of 5-fluorouracil: Water-assisted proton transfer. J Phys Chem A 2005;109(9):1981–1988.

[27] Alagona G, Ghio C. Keto-enol tautomerism in linear and cyclic $\beta$-diketones: A DFT study in vacuo and in solution. Int J Quantum Chem 2008;108(10):1840–1855.

[28] Huang X, Tang C, Li J, Chen LC, Zheng J, Zhang P, et al. Electric field–induced selective catalysis of single-molecule reaction. Sci Adv 2019;5(6):eaaw3072.

[29] Shi FQ, Li X, Xia Y, Zhang L, Yu ZX. DFT study of the mechanisms of in water Au (I)-catalyzed tandem [3, 3]-rearrangement/Nazarov reaction/[1, 2]-hydrogen shift of enynyl acetates: a proton-transport catalysis strategy in the water-catalyzed [1, 2]-hydrogen shift. J Am Chem Soc 2007;129(50):15503–15512.

[30] Stuyver T, Shaik S. Promotion energy analysis predicts reaction modes: nucleophilic and electrophilic aromatic substitution reactions. Journal of the American Chemical Society 2021;143(11):4367–4378.

[31] Joy J, Stuyver T, Shaik S. Oriented external electric fields and ionic additives elicit catalysis and mechanistic crossover in oxidative addition reactions. J Am Chem Soc 2020;142(8):3836–3850.

[32] Harrop TC, Mascharak PK. In: Kretsinger RH, Uversky VN, Permyakov EA, editors. Cobalt-containing Enzymes New York, NY: Springer New York; 2013. p. 684–690. https://doi.org/10.1007/978-1-4614-1533-6_71.

[33] Zhao Q, Vaddadi SM, Woulfe M, Ogunfowora LA, Garimella SS, Isayev O, et al. Comprehensive exploration of graphically defined reaction spaces. Sci Data 2023;10(1):145.

[34] Grambow CA, Pattanaik L, Green WH. Reactants, products, and transition states of elementary chemical reactions based on quantum chemistry. Sci Data 2020;7(1):137.

[35] Grambow CA, Pattanaik L, Green WH. Deep learning of activation energies. J Phys Chem Lett 2020;11(8):2992–2997.

[36] Spiekermann K, Pattanaik L, Green WH. High accuracy barrier heights, enthalpies, and rate coefficients for chemical reactions. Sci Data 2022;9(1):417.

[37] Stuyver T, Jorner K, Coley CW. Reaction profiles for quantum chemistry-computed [3+ 2] cycloaddition reactions. Sci Data 2023;10(1):66.

[38] Stuyver T, Coley CW. Machine Learning-Guided Computational Screening of New Candidate Reactions with High Bioorthogonal Click Potential. Chem Eur J 2023;p. e202300387.

[39] Pattanaik L, Ingraham JB, Grambow CA, Green WH. Generating transition states of isomerization reactions with deep learning. Phys Chem Chem Phys 2020;22(41):23618–23626.

[40] Schreiner M, Bhowmik A, Vegge T, Busk J, Winther O. Transition1x-a dataset for building generalizable reactive machine learning potentials. Sci Data 2022;9(1):779.

[41] Duan C, Du Y, Jia H, Kulik HJ. Accurate transition state generation with an object-aware equivariant elementary reaction diffusion model. arXiv preprint arXiv:230406174 2023;.

[42] Weininger D. SMILES, a chemical language and information system. 1. Introduction to methodology and encoding rules. J Chem Inf Comput 1988;28(1):31–36.

[43] Coley CW, Jin W, Rogers L, Jamison TF, Jaakkola TS, Green WH, et al. A graph-convolutional neural network model for the prediction of chemical reactivity. Chem Sci 2019;10(2):370–377.

[44] Bannwarth C, Ehlert S, Grimme S. GFN2-xTB—An accurate and broadly parametrized self-consistent tight-binding quantum chemical method with multipole electrostatics and density-dependent dispersion contributions. J Chem Theor Comput 2019;15(3):1652–1671.

[45] Landrum G, et al. RDKit: A software suite for cheminformatics, computational chemistry, and predictive modeling. Greg Landrum 2013;8:31.

[46] Frisch Me, Trucks G, Schlegel H, Scuseria G, Robb M, Cheeseman J, et al., Gaussian 16, revision C. 01. Gaussian, Inc., Wallingford CT; 2016.

[47] Jensen MKMJH, xtb_gaussian; 2020. https://github.com/jensengroup/xtb_gaussian/blob/main/xtb_external.py.

[48] Zimmerman P. Reliable transition state searches integrated with the growing string method. J Chem Theor Comput 2013;9(7):3043–3050.

[49] Zimmerman PM. Automated discovery of chemically reasonable elementary reaction steps. J Comput Chem 2013;34(16):1385–1392.

[50] Legault C, CYLview, 1.0 b. Université de Sherbrooke Canada; 2009.

[51] Maeda S, Morokuma K. Finding reaction pathways of type A+ B→ X: Toward systematic prediction of reaction mechanisms. J Chem Theor Comput 2011;7(8):2335–2345.

[52] Tomasi J, Mennucci B, Cammi R. Quantum mechanical continuum solvation models. Chem Rev 2005;105(8):2999–3094.

[53] Marenich AV, Cramer CJ, Truhlar DG. Universal solvation model based on solute electron density and on a continuum model of the solvent defined by the bulk dielectric constant and atomic surface tensions. J Phys Chem B 2009;113(18):6378–6396.

[54] Mandal D, Ramanan R, Usharani D, Janardanan D, Wang B, Shaik S. How does tunneling contribute to counterintuitive H-abstraction reactivity of nonheme Fe (IV) O oxidants with alkanes? J Am Chem Soc 2015;137(2):722–733.

[55] Shaik S, Shurki A. Valence bond diagrams and chemical reactivity. Angew Chem, Int Ed 1999;38(5):586–625.

[56] Shaik SS, Hiberty PC. A chemist's guide to valence bond theory. John Wiley & Sons; 2007.

[57] Stuyver T, Shaik S. Resolving entangled reactivity modes through external electric fields and substitution: Application to E2/SN2 reactions. J Org Chem 2021;86(13):9030–9039.

[58] Toniato A, Unsleber JP, Vaucher AC, Weymuth T, Probst D, Laino T, et al. Quantum chemical data generation as fill-in for reliability enhancement of machine-learning reaction and retrosynthesis planning. Digital Discovery 2023;2(3):663–673.

[59] Behler J, Parrinello M. Generalized neural-network representation of high-dimensional potential-energy surfaces. Phys Rev Lett 2007;98(14):146401.

[60] Staub R, Gantzer P, Harabuchi Y, Maeda S, Varnek A. Challenges for Kinetics Predictions via Neural Network Potentials: A Wilkinson's Catalyst Case. Molecules 2023;28(11):4477.

[61] Duan C, Janet JP, Liu F, Nandy A, Kulik HJ. Learning from failure: predicting electronic structure calculation outcomes with machine learning models. J Chem Theor Comput 2019;15(4):2331–2345.

[62] Nakao A, Harabuchi Y, Maeda S, Tsuda K. Exploring the Quantum Chemical Energy Landscape with GNN-Guided Artificial Force. J Chem Theor Comput 2023;19(3):713–717.

## GRAPHICAL ABSTRACT

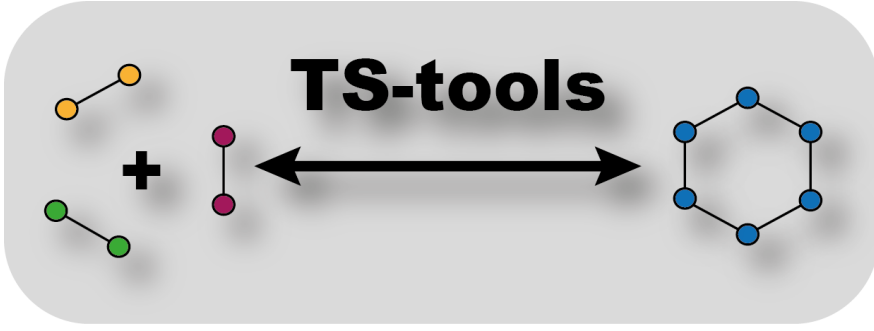


TS-tools facilitates the automated localization of transition states (TS) based on a textual reaction SMILES input. On a benchmarking dataset of mono- and bimolecular reactions, TS-tools reaches an excellent success rate of 95% already at xTB level of theory. For tri- and multimolecular reaction pathways – which are typically not benchmarked when developing new TS search approaches – TS-tools retains its ability to identify TS geometries, though a DFT treatment becomes essential in many cases.